

# Advances in understanding imbibition characteristics of shale using an NMR technique: a comparative study of marine and continental shale

Liu Yang<sup>1,2,7</sup> , Ninghui Dou<sup>3</sup>, Xiaobing Lu<sup>2</sup>, Xuhui Zhang<sup>2,7</sup>, Xu Chen<sup>4</sup>, Jian Gao<sup>4</sup>, Chengwei Yang<sup>5</sup> and Yang Wang<sup>6</sup>

<sup>1</sup> State Key Laboratory for Geomechanics and Deep Underground Engineering, China University of Mining and Technology, 100083 Beijing, People's Republic of China

<sup>2</sup> Key Laboratory for Mechanics in Fluid Solid Coupling Systems, Institute of Mechanics, Chinese Academy of Sciences, 100190 Beijing, People's Republic of China

<sup>3</sup> Sinopec Research Institute of Petroleum Engineering, 100101 Beijing, People's Republic of China

<sup>4</sup> Research Institute of Petroleum Exploration and Development, Beijing, 100083, People's Republic of China

<sup>5</sup> Exploration & Development Research Institute, Petro China Changqing Oilfield Company, 136201 Xi'an, People's Republic of China

<sup>6</sup> Shanxi Key Laboratory of Advanced Stimulation Technology for Oil & Gas Reservoirs, Xi'an, People's Republic of China

E-mail: [shidayangliu@126.com](mailto:shidayangliu@126.com) (Liu Yang) and [zhangxuhui@imech.ac.cn](mailto:zhangxuhui@imech.ac.cn) (Xuhui Zhang)

Received 5 November 2017, revised 2 February 2018

Accepted for publication 15 February 2018

Published 25 April 2018



## Abstract

Studying the imbibition characteristics of shale contributes to understanding the low flowback efficiency (<20%) and its potential effects on gas production. Previous studies have mainly focused on imbibition characteristics of marine shale, but few investigations have been conducted on continental shale to explore the microscopic imbibition mechanism. This paper performs a series imbibition experiments on typical sandstone, marine, and continental shale samples. The water migration and distribution is monitored by the nuclear magnetic resonance technique. For the same type of shale (marine or continental shale), the imbibition rate has a positive relationship with the clay mineral content. But continental shale contains more clay minerals and has a larger imbibition rate than marine shale. The expansion of clay minerals may have different impacts on the pore structure of marine and continental shale as the T<sub>2</sub> spectra present. In contrary to non-swelling sandstone with constant T<sub>2</sub> values, the T<sub>2</sub> values of marine and continental shale vary during water imbibition. The T<sub>2</sub> values of marine shale increase gradually due to the extension of microfractures, which can enhance the water imbibition rate and gas flowing channels significantly. However, the T<sub>2</sub> values of continental shale decrease gradually as a result of destruction of matrix pores, which can decrease the water imbibition rate and have negative effects on gas flow channels. Compared with continental shale, the low flowback efficiency induced by water imbibition may be more suitable for marine shale to get good shale gas production. These findings can help understand the special imbibition characteristics of marine and continental shale.

Keywords: marine shale, continental shale, imbibition, clay minerals, NMR

(Some figures may appear in colour only in the online journal)

<sup>7</sup> Authors to whom any correspondence should be addressed.

## 1. Introduction

Shale gas has become an important energy supply to meet the demands of oil and gas in the USA and Canada. Because of the ultra-low porosity and permeability in shale gas, large scale multi-stage fracturing has been widely applied for the effective development of shale gas (Odumabo and Karpyn 2014). Recent studies show that a large fraction of injected fluid volume is retained in fractured shale reservoirs, leading to extremely low flowback efficiency (<20%). The fracturing fluid imbibition into matrix pores has been regarded as the primary mechanism for inefficient water recovery in shale gas. The interactions between shale and water have positive or negative effects on gas production, which has gained more and more attention (Dehghanpour *et al* 2013, Meng *et al* 2016). A deep understanding of shale imbibition characteristics is significant for optimal shutting-in periods after fracturing operations (Hayatdavoudi *et al* 2015).

Spontaneous imbibition is a process whereby non-wetting liquid is spontaneously replaced by wetting liquid driven by capillary pressure. Lucas (1918) and Washburn (1921) proposed that the imbibition height and time have the relationship of  $\sqrt{t}$  in a capillary tube. Considering the special imbibition characteristics of shale, there is great controversy over the validity of the Lucas–Washburn model for shale in recent years. Attempts to understand the deviation from classical imbibition theory and explore several alternative models have received increasing attention. Hu *et al* (2012) pointed out that the time exponent is lower than 0.5, suggesting low pore connectivity in Barnett shale matrix. But the capillary pressure and viscous drag cannot explain this deviation (Lam and Horváth 2000). In particular, shale develops micro/nano pores, and the water imbibition in nanoporous media is of scientific and technological interest (Gruener *et al* 2016).

The fracturing fluid imbibition mechanism has been investigated. In a conventional reservoir, the water is imbibed into pores due to capillary pressure. Nevertheless, the driving force of imbibition is capillary pressure and osmotic pressure in shale reservoirs (Dehghanpour *et al* 2012). The osmotic pressure plays a greater role in clay-rich shale than capillary pressure does, and the matrix pores can imbibe volumes of fluid larger than its porous volume measured by helium (Ge *et al* 2015). The pore pressure in shale matrix can be enhanced from powerful imbibition effects, leading to the generation of microfractures (Wang and Raman 2015). Cheng *et al* (2015) proposed that the microfractures can significantly increase the imbibition rate due to surface spreading on a rough fracture face. In addition, both clay minerals and organic material are developed in organic shale, and the mix-wettability also has a great influence on imbibition characteristics (Dehghanpour *et al* 2012). Meng *et al* (2016) monitored the co-current and counter-current imbibition of volcanic rock and marine shale by using the nuclear magnetic resonance (NMR) technique, suggesting that some preferential pores for water imbibition may exist among shale matrix pores.

In China, marine shale of the southern Sichuan Basin has achieved commercial production. The less prospective continental shale of the Erdos Basin is receiving increasing attention. Compared with marine shale, continental shale has more clay minerals and a more complex pore structure. At present, few studies have been conducted to explore the imbibition characteristics of continental shale. In this work, water co-current imbibition experiments are conducted on sandstone, marine, and continental shale samples. The low-field NMR technique is used to monitor the water migration and distribution characteristics during water imbibition. In discussing and extending the experimental results this paper aims to understand shale imbibition characteristics and its potential effects on gas production.

## 2. Materials and methods

### 2.1. Experimental samples

The shale samples were collected from typical shale formations of the Sichuan Basin, Ordos Basin, and Qaidam Basin. The Sichuan Basin is the greatest potential area for marine shale gas production in China. Te Fuling District in Chongqing City, focused on the Longmaxi formation, has realized great breakthroughs. The continental shale formations (Lower Chang 7 and Ganchaigou) are part of the Ordos Basin and the Qaidam Basin, respectively, which are hot targets for continental shale gas exploration. At present, they are still at the initial stage of exploration and development. The basic information on different reservoirs is listed in table 1. The sandstone that is known to be of low clay content and high permeability is selected for the calibration standard.

The bulk mineralogical compositions of the samples are presented in table 2, which are obtained from x-ray diffraction patterns following the measurement standard of SY/T5163-2010. The test is conducted at the State Key Laboratory of Petroleum Resources and Prospecting at the China University of Petroleum, Beijing. The five shale formations are characterized by a high concentration of clay (20.5%–48.2%) and quartz (29.3%–38.3%). The clay minerals contain mainly illite and I/S (illite/smectite mixed-layer). Guo *et al* (2015) illustrated the application of a mineralogical method to calculate the shale brittleness index. More brittle shale contributes to forming the fracture network after fracturing operations. Marine shale with a higher brittleness index is characterized by well developed organic pores and microfractures (figure 1(a)). In continental shale with a lower brittleness index, the organic pores are not well developed, which tends to be accompanied by clay minerals (figure 1(b)). Considering the different clay mineral content in marine and continental shale, comparative experiments can be performed to study the effects of clay mineral content on water imbibition characteristics.

The table 3 presents the physical parameters of samples. The measurement of porosity and permeability is carried out on the cylindrical plugs of 2.5 cm diameter. Considering the

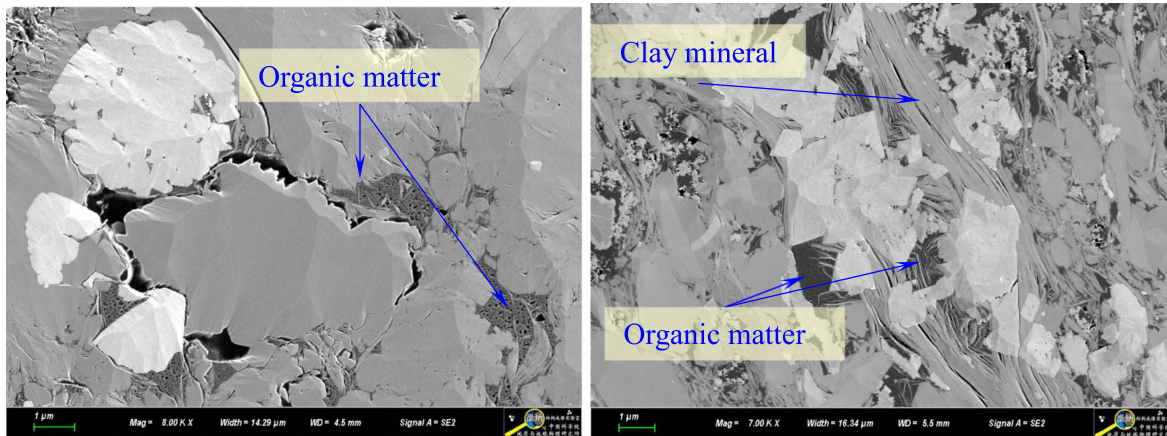


**Figure 1.** Scanning electron microscopy (SEM) images: (a) marine shale-LJP and (b) continental shale-GCG.

**Table 1.** Tight reservoir characteristics.

Label	Formation	Lithology	Depositional environment	Source
LJP	Lujiaoping	Shale	Marine	Sichuan Basin
LMX	Longmaxi	Shale	Marine	Sichuan Basin
NTT	Niutitang	Shale	Marine	Sichuan Basin
LYC	Lower Chang 7	Shale	Continental	Erdos Basin
GCG	Ganchaigou	Shale	Continental	Qaidam Basin
LCG	Lucaogou	Tight sandstone		Junggar Basin
SHZ	Shihezi	Conventional sandstone		Erdos Basin

**Table 2.** XRD mineralogy results.

Label	Mineral composition, wt. %					Clay abundance relative to total clay, wt. %				
	Quartz	Calcite	Feldspar	Dolomite	Clay	Illite	Smectite	I/S	Chlorite	Kaolinite
LJP	30.2	22.5	9.2	14.4	23.7	20.1	5.2	54.5	9.6	10.6
LMX	38.3	5.5	10.8	15.2	30.2	14.3	3.8	65.1	10.3	6.5
NTT	30.2	12.3	21.5	15.5	20.5	2.2	4.4	74.0	19.4	0
LYC	29.3	8.5	15.8	9.6	36.8	13.2	1.6	63.9	11.3	10.0
GCG	33.2	8.2	10.4	0	48.2	10.5	1.2	85.2	3.1	0
LCG	12.0	0	22.1	58.7	7.2	12	80	0	5	3
SHZ	28.5	8.1	28.7	23.5	11.2	95.3	0	4.7	0	0

fact that the slick water has been widely used as fracturing fluid in shale gas, deionized (DI) water is selected as the imbibed fluid for imbibition tests.

## 2.2. NMR measurement equipment

NMR, a non-destructive technique, can detect the content of protons (hydrogen H) of fluid in the porous media, which is an efficient method to acquire the physical characteristics of rocks (e.g. porosity, water saturation, permeability, and pore size distribution (PSD)). Generally, transverse relaxation time (T2) spectra of NMR are applied widely in the areas of laboratory and logging applications. As for T2 spectra, the

fluid in the larger pores has a longer T2 relaxation time and that in the smaller pores has a shorter T2 relaxation time. In addition, more fluid in a certain pore corresponds to a larger signal amplitude. Based on this principle, T2 spectra can help analyze the fluid content of different pores during water imbibition (Meng *et al* 2016).

It should be noted that the instrument parameters in the CPMG sequence involves a waiting time (RD), echo numbers (NECH), signal superposition times (SCANS), and echo time interval ( $T_E$ ), which significantly influence the measurement accuracy (Xu *et al* 2015). A too short RD results in a loss of information from large pores, but a too long RD could increase the measurement time. An RD of >3000 ms is

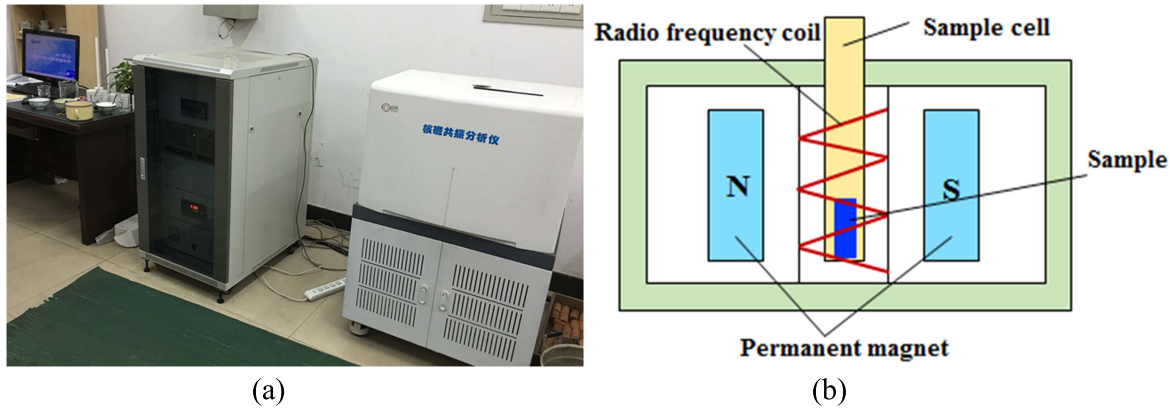


**Figure 2.** Low-field NMR measurement equipment: (a) physical map and (b) schematic diagram.

**Table 3.** Basic properties of core plugs for NMR experiments.

No.	Diameter, cm	Length <i>L</i> , cm	Permeability <i>K</i> , mD <sup>a</sup>	Porosity $\Phi$ , % <sup>b</sup>	Final spectra area variation (SAV)	Final imbibed water (IW), g	SAV/IW, 1/g
LJP	2.49	2.3	0.0032	3.1	6454	0.301	21 230
LMX	2.51	2.1	0.0054	2.8	11 545	0.652	17 762
NTT	2.50	3.7	0.0028	1.5	7562	0.351	21 362
LYC	2.50	2.1	0.0020	1.3	1141	0.062	18 704
GCG	2.50	1.3	0.0025	1.2	3445	0.181	19 138
LCG	2.50	1.5	0.0092	8.5	9101	0.424	21 515
SHZ	2.52	5.1	2.1	12.2	34 509	1.792	19 289

<sup>a</sup> The pulse decay permeability is measured at the test temperature of 25 °C, confining pressure of 8 MPa, and pore pressure of 5 MPa). The pulse decay permeability apparatus was manufactured by Yongruida Technology Co, Ltd of Beijing, China.

<sup>b</sup> At the test temperature of 25 °C and pressure of 200 psi, the samples' porosity is measured by a helium porosimeter.

suitable for sandstone, and >8000 ms is suitable for shale embedded with microfractures. Similarly, larger NECH and SCANS favor measurement accuracy, which are 2048 and 64, respectively, in this study. In addition, if the  $T_E$  (the time intervals between two pulses of sequential 180-degrees) is larger than 0.3 ms, the fluid signal in small pores will not be complete. As for the low-field NMR equipment, the minimum value of  $T_E$  is 0.3 ms. Therefore, the T2 relaxation time of some ultra-micropores tends to be distinguished, and the whole pore distribution obtained by T2 spectra is incomplete. NMR measurement equipment (MiniMR-VTP, Suzhou Niumag Analytical Instrument Corporation) can provide a magnetic field intensity of 0.5 T (figure 2). The testing environment conditions included a temperature of 25 °C, humidity of 40%, and atmospheric pressure of 0.1 MPa.

According to Gomaa *et al* (2014), the T2 relaxation time in the rocks can be given by

$$\frac{1}{T_2} = \rho_2 \frac{S}{V},$$

where  $\rho_2$  is the surface relaxivity,  $S$  is the surface area, and  $V$  is the pore volume.

Assuming the pores are tube shape, the pore radius  $r$  can be written as function of  $T_2$ .

$$r = 2\rho_2 T_2.$$

Therefore, the  $T_2$  spectra from NMR tests could indicate the characteristics of the PSD. The pore radius has a positive relationship with the  $T_2$  value.

### 2.3. Experimental procedure

The spontaneous imbibition process is monitored by low-field NMR equipment to measure the water gain in the pores. The experimental procedures are listed below.

- (1) Dry the samples at 105 °C until there is no further weight change, and measure the initial weight and size of the samples.
- (2) Start the NMR apparatus and warm-up for an hour prior to the experiments.
- (3) Place the sample in the cell (figure 2(b)) and determine the  $T_2$  spectra of dry samples.
- (4) Immerse one end face of the shale samples into water (2 mm depth) to conduct co-current imbibition experiments. After a period of time, wipe the water from the

Sample	LJP	LMX	NTT	LYC	GCG	LCG
Before						
After						

**Figure 3.** Photographs of samples before and after exposure to DI water.

sample surface using absorbent paper, measure the weight, and determine the T2 spectra.

- (5) Repeat step (4) at the selected time intervals. The time intervals are shorter at the early period, and longer at the late stage, as the change in sample weight at the beginning is much quicker than that at the late period.

than large pores. In addition, the rate of peak area change is larger at the beginning and smaller in the late period, which illustrates that the rate of imbibed volume decreases as a function of time.

**3.2.1. Conventional and tight sandstone.** The conventional and tight sandstone samples could be considered as the calibration standard to understand the imbibition characteristics of shale samples. In figures 4(a) and (b), the trend lines are perpendicular to the  $x$ -axis, indicating that the T2 values do not vary with soaking time. The water is imbibed into the sandstone pores uniformly in the whole pore range. In addition, the trend line in conventional sandstone corresponds to 1.2 ms and that in tight sandstone corresponds to 0.5 ms, indicating that the conventional sandstone has a much larger pore size than the tight sandstone. It seems consistent with larger porosity and permeability in conventional sandstone, as shown in table 3.

Due to the special pore structure and mineral composition of shale, the Handy imbibition model may not be applicable for shale. But the qualitative analysis based on the Handy model is still convincing (Makhanov *et al* 2012). According to the Handy model, the imbibed volume is directly proportional to the square root of time (Handy 1960). In figure 5, the imbibed water mass and spectra area variation as a function of  $\sqrt{t}$  are presented, which have the similar trend. As expected, both the imbibed mass and spectra area variation are approximately proportional to  $\sqrt{t}$ , as described by the Handy model. It suggests that the low-field NMR machine is reliable for monitoring water imbibition. The amplitude signal measured by NMR is indeed representative of the imbibed water. According to figure 5, the NMR amplitude signal of 1 g of DI water corresponds to about a 20 000 spectra area as shown in table 3. The imbibed mass of conventional sandstone sample is about 1.672 g at 7 h, but the imbibed mass of tight sandstone sample is about 0.423 g at 7.8 h. The conventional sandstone sample has a much larger

### 3. Experimental results

#### 3.1. Macroscopic observations of samples before and after water imbibition

Figure 3 shows pictures of the LJP, LMX, NTT, LYC, GCG, and LCG formation samples before and after exposure to DI water. A rather large difference exists among the rock surfaces of different formation samples. The shale samples are black and composed of extremely small and uniform grains. No obvious change is observed on the surface of the LJP, NTT, LYC, and LCG formation samples. Only the surface color became much darker after exposure to DI water. However, great changes appeared on the surface of the LMX and GCG samples. Cracks were observed on the surface of LMX, which were parallel to the bedding plane. The GCG sample disintegrated completely after exposure to DI water.

#### 3.2. Water imbibition characteristics of different rock samples

Figures 4, 6, and 8 show the T2 spectra evolution of different rocks during water imbibition. All the time labels listed in the figures represent accumulative soaking time. Similar overall characteristics are found in the curves of the T2 spectra. The T2 spectra of all the formation samples have two peaks and the area of the left peak is much larger than that of the right peak. The right peak area remains almost constant, but the left peak area increases to outweigh the right peak area finally. It suggests that small pores have a much higher volume fraction

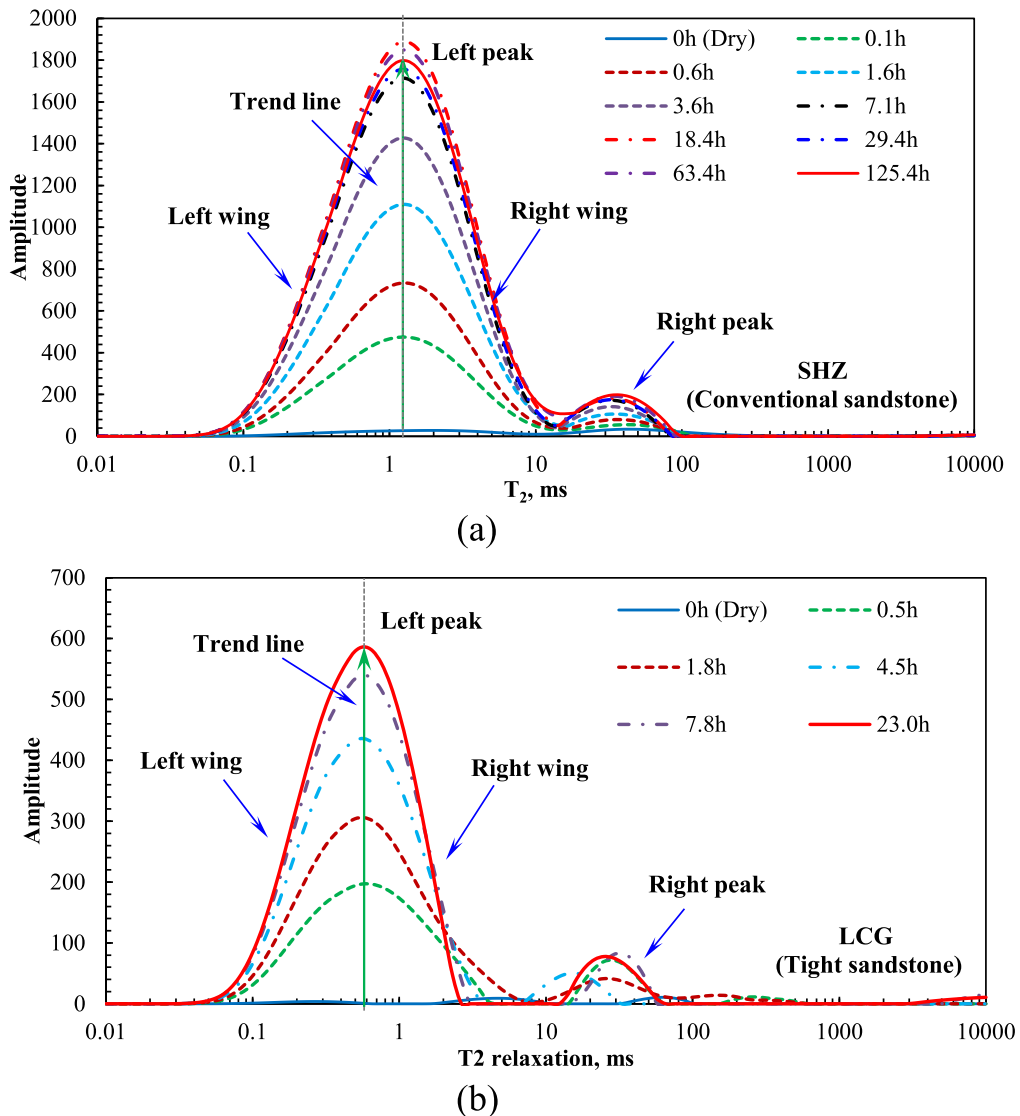


**Figure 4.** The NMR T<sub>2</sub> spectra of the SHZ and LCG samples during water imbibition: (a) SHZ sample and (b) LCG sample. The spectra on the left side of the dashed black line represent the left wing and the spectra on the right side of the dashed black line represent the right wing. The green arrow represents trend line.

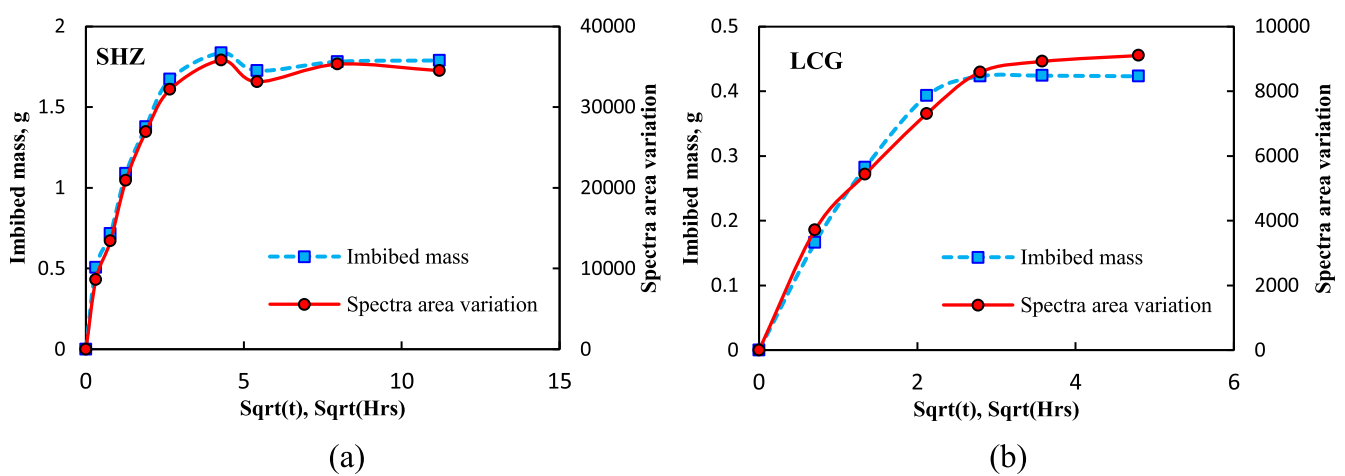


**Figure 5.** Comparison between the imbibed mass versus  $\sqrt{t}$  and spectra area variation versus  $\sqrt{t}$ : (a) SHZ sample and (b) LCG sample.

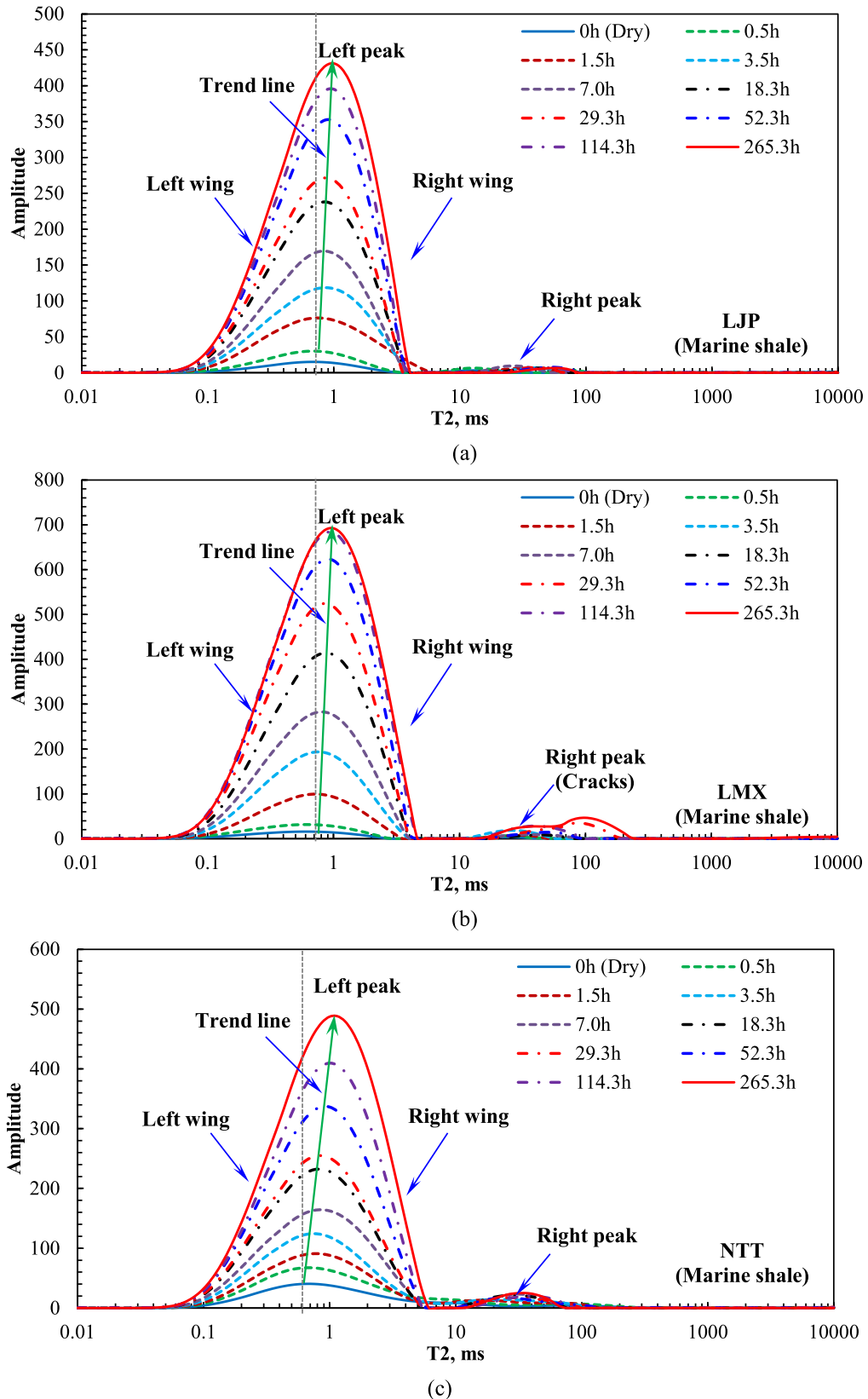


**Figure 6.** NMR T2 spectra of the LJP, LMX, and NTT samples during water imbibition: (a) LJP sample, (b) LMX sample, and (c) NTT sample.

imbibition rate than that of the tight sandstone, which can be explained by the better physical characteristics of conventional sandstone.

**3.2.2. Marine shale.** In figures 6(a)–(c), the isolated bimodal peaks are observed in the T2 spectra of the marine shale samples, and the right peak area is too small to

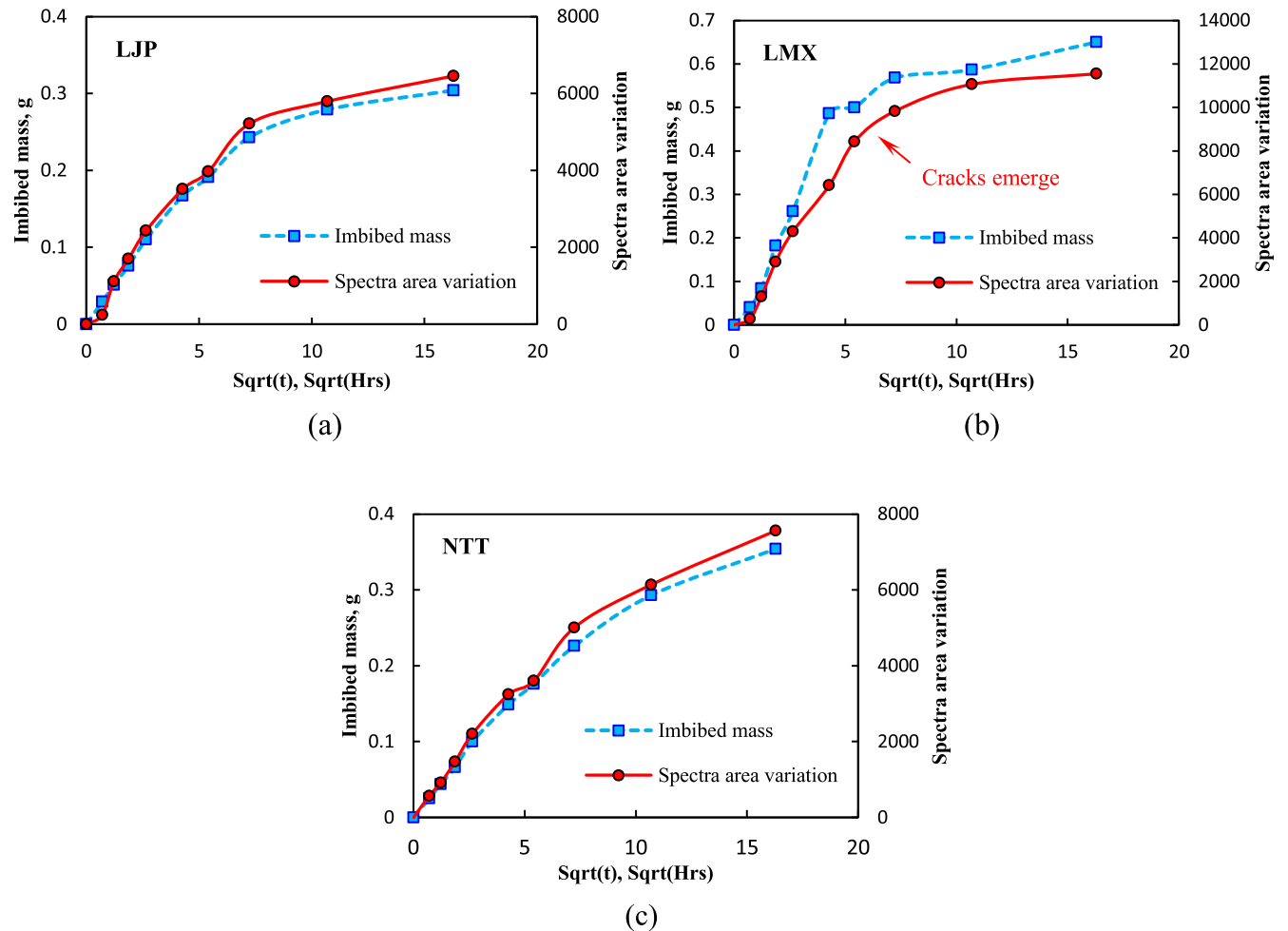


**Figure 7.** Comparison between the imbibed mass versus  $\sqrt{t}$  and spectra area variation versus  $\sqrt{t}$ : (a) LJP sample, (b) LMX sample, and (c) NTT sample.

be diagnosed. The trend lines are not perpendicular to the  $x$ -axis but incline gently to the right. The spectra area difference between the right wing and left wing increases gradually, which indicates that new larger pores or microfractures may occur during water imbibition. The right peak of the LMX sample increases significantly (figure 6(b)), which is consistent with the cracks observed after exposure to water as shown in figure 3. It can be speculated that the T2 spectra incline of marine shale is induced by microfracture propagation. As for the LJP and NTT samples, the microfractures could not connect to one another to form larger cracks visible to the naked eye. They can only enhance the right wing of the left peak.

For the LJP, LMX, and NTT marine shale, the imbibed water mass and spectra area variation as a function of  $\sqrt{t}$  are presented in figure 7. Compared with sandstone, the imbibition curves indicate ‘upward tails’ in the late stage of imbibition. It suggests that marine shale needs a longer time to reach an equilibrium state due to its

complex pore structure (Yang et al 2016). At 29.3 h, the imbibed mass of LJP, LMX, and NTT are 0.191, 0.501 and 0.176 g, respectively. The LJP shale has a larger imbibition rate compared to the NTT shale but has a smaller imbibition rate compared to the LMX shale. It can be explained by the higher clay mineral content in the LMX and LJP shale. Besides the capillary pressure, water adsorption due to clay minerals can act as the additional driving force to increase the imbibition rate.

**3.2.3. Continental shale.** In figures 8(a) and (b), the T2 spectra behaviors of continental shale are different from those of sandstone and marine shale. Surprisingly, the trend lines of the LYC and GCG samples incline gently to the left. The spectra area difference between the right wing and the left wing decreases gradually, which indicates that new smaller pores may occur during water imbibition. Considering the disintegration of the GCG sample after exposure to DI water, the authors speculate that the new

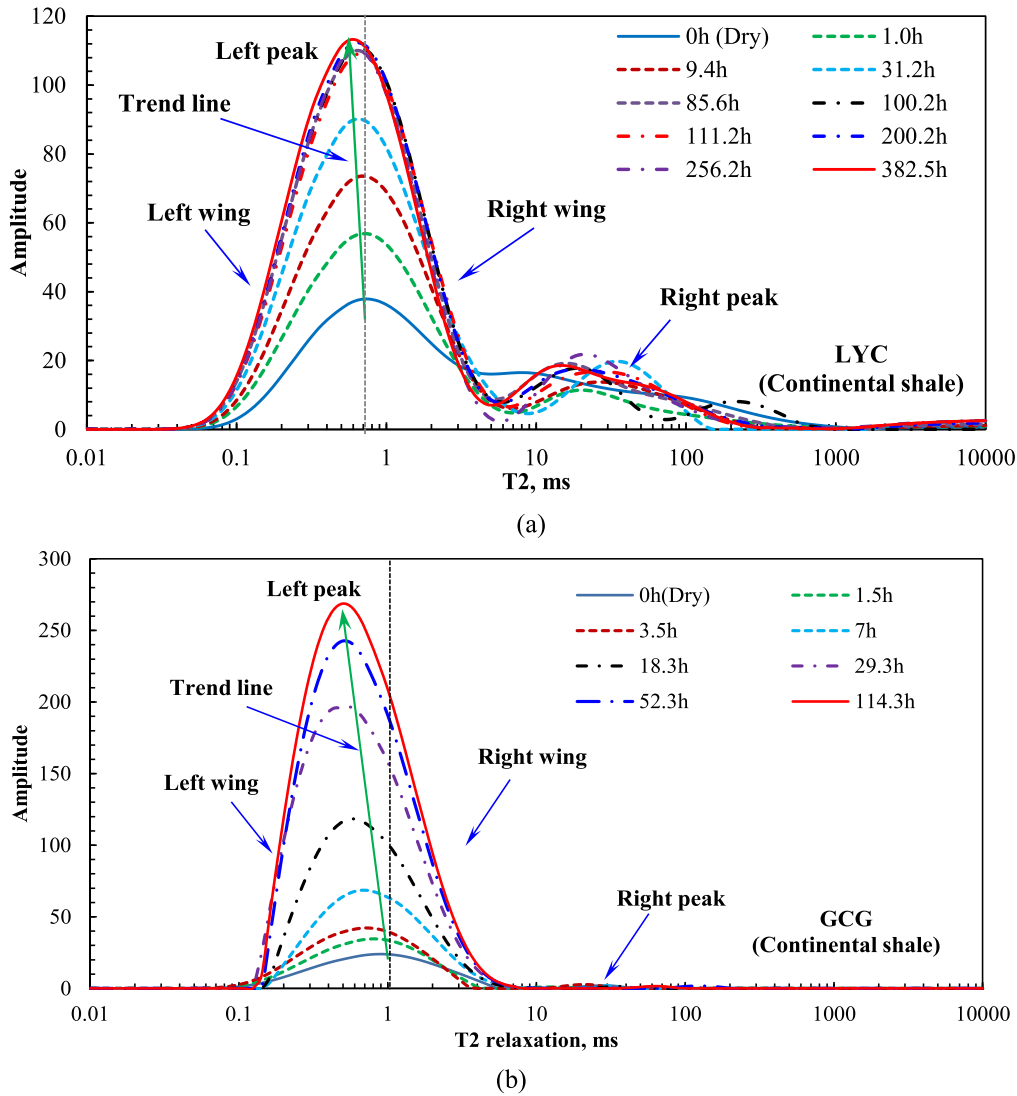


**Figure 8.** NMR T2 spectra of the LYC and GCG samples during water imbibition: (a) LYC sample and (b) GCG sample.

smaller pores of the LYC and GCG samples may be related to super-high clay mineral content. Continental shale formation of LYC and GCG have a much higher clay content ( $>36.8\%$ ) and the high swelling pressure tends to compact or destroy matrix pores to induce water sensitive damage.

For the LYC and GCG continental shale, the imbibed water mass and spectra area variation as a function of  $\sqrt{t}$  are presented in figure 9. Compared with sandstone, the imbibition curves also indicate ‘upward tails’ in the late stage of imbibition. In addition, the imbibed mass of the GCG shale sample is about 0.141 g at 29.3 h, but the imbibed mass of the LYC shale sample is about 0.042 g at 31.2 h. The GCG shale sample has a much larger imbibition rate than the LYC shale sample, which can also be explained by the high clay mineral content in GCG shale.

**3.2.4. Comparison of imbibition characteristics of sandstone, marine, and continental shale.** In order to advance the

understanding of the imbibition characteristics of shale, comparative studies on T2 spectra and imbibition rate are conducted on sandstone, marine, and continental shale.

**3.2.4.1. Comparison of T2 spectra characteristics.** The T2 values of the left peak tops can reflect the T2 spectra behaviors of different rocks. Figure 10(a) presents the relationship between the peak position variation (PPV) and imbibition time. The PPV values of conventional and tight sandstone are zero, suggesting that no new pores occur and the water is imbibed uniformly into the pores. The PPV values of marine shale are positive, demonstrating that new larger pores (microfractures) may occur during water imbibition. The NTT marine shale has the highest PPV values and LMX marine shale has the lowest PPV values. In addition, the PPV value of continental shale is negative, indicating that new smaller pores may occur during water imbibition. The PPV value of GCG continental shale is smaller than that of LYC continental shale. It is worth noting that the maximum PPV values are inversely

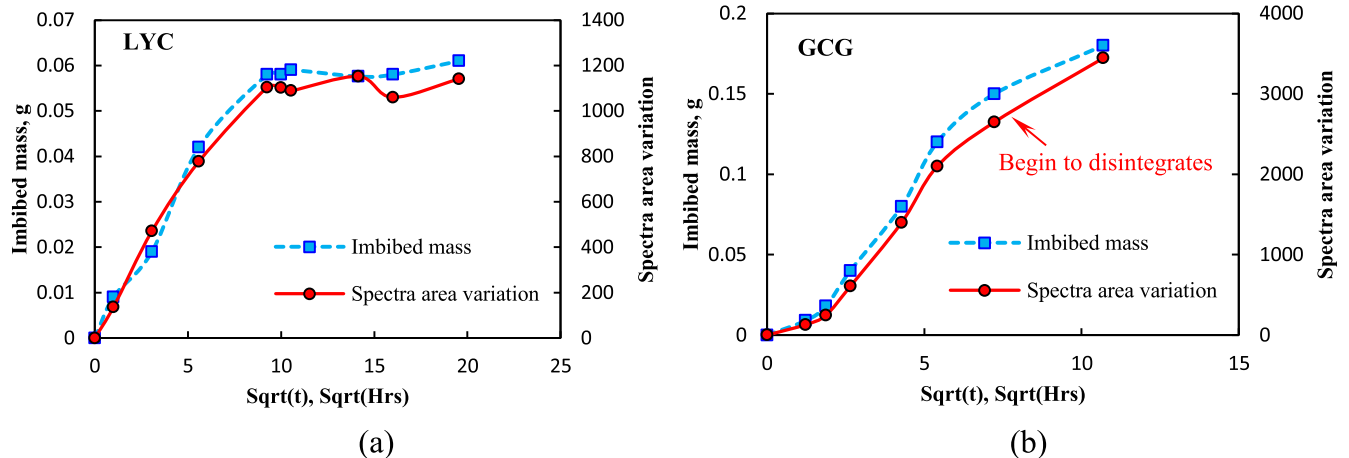


**Figure 9.** The comparison between the imbibed mass versus  $\sqrt{t}$  and spectra area variation versus  $\sqrt{t}$ : (a) LYC sample and (b) GCG sample.

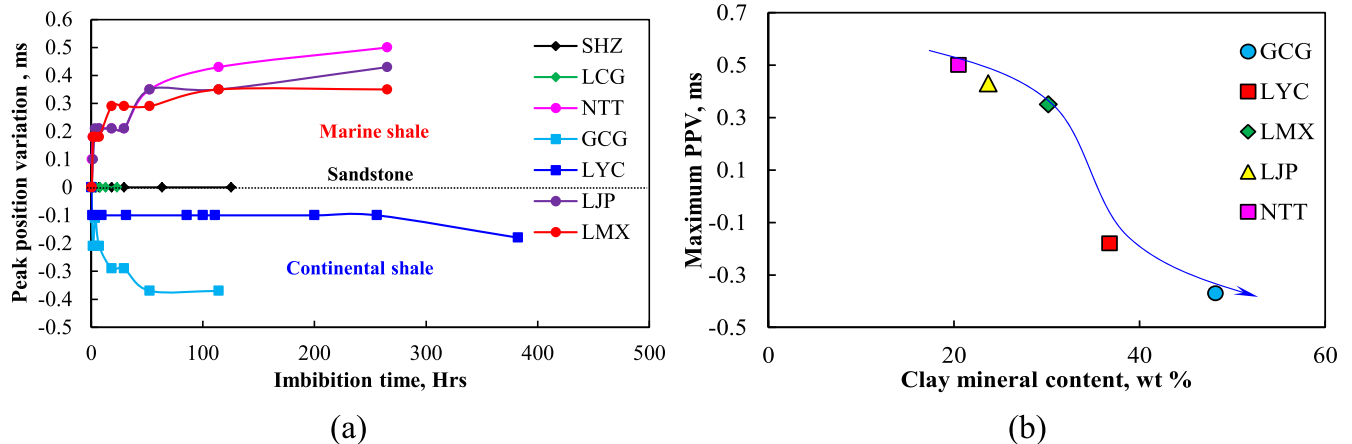


**Figure 10.** Curves of PPV versus imbibition time and maximum PPV versus clay content: (a) PPV versus imbibition time and (b) maximum PPV versus clay content.

proportional to the clay mineral content of shale (i.e., marine and continental shale). The more clay minerals the shale has, the smaller the maximum PPV values become (figure 10(b)).

**3.2.4.2. Comparison of imbibition rates.** According to the Handy model (Handy 1960), the slope of imbibition curves represent the imbibition rate. As a result of high permeability and porosity, the imbibition rate of conventional and tight sandstone is larger than that of marine and continental shale (figure 11(a)). For the same type of shale (marine or continental shale), the imbibition rate has a positive relationship with the clay mineral content (figure 11(b)). However, the imbibition rate of marine shale is larger than that of continental shale in spite of a much higher clay content in continental shale (figure 11(b)). The discrepancy can be explained by the different effects of clay mineral expansion on the pore structure of marine and continental shale as the T2 spectra present. In marine shale, water imbibition can induce

microfracture propagation to improve the physical characteristics, which significantly enhances the imbibition rate. Nevertheless, too much clay mineral in continental shale can compact the matrix pores and induce water sensitive damage during water imbibition, which decreases the imbibition rate.

#### 4. Discussion

To a large extent, the different T2 spectra behaviors tend to be determined by clay mineral content. Three simplified types are proposed depending on the series of experiments in this study and our previous studies (Yang et al 2015, 2016). The type of model could contribute to the comprehension of special imbibition characteristics, and provide a reference to optimize shutting-in periods in shale gas. The authors classify these models based on the capacity of clay minerals swelling.

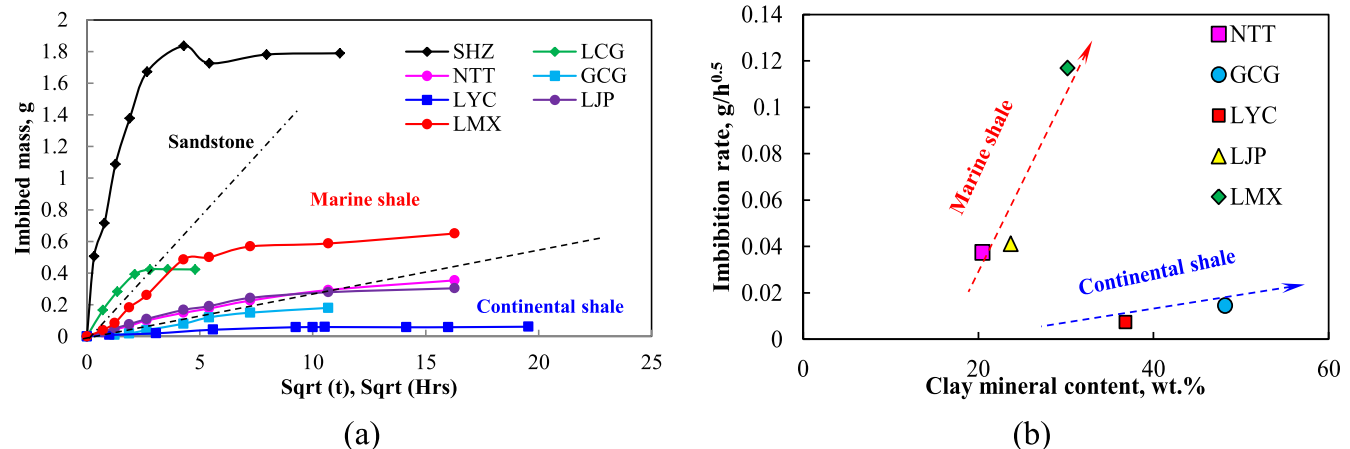


**Figure 11.** Curves of the imbibed mass versus  $\sqrt{t}$  and imbibition rate versus clay mineral content: (a) imbibed mass versus  $\sqrt{t}$  and (b) imbibition rate versus clay mineral content.

If the clay mineral content is very low, the clay minerals tend to be suspended by brittle minerals (figure 12(a)). The tensile strength of rocks is large due to high content of brittle minerals. The swelling pressure of clay minerals is so small that it cannot exceed the tensile strength. The pore structure of rocks could not change during water imbibition. The T2 spectra that represent pore size tend to remain constant. According to the experimental results of the SHZ and LXG samples, the rocks may have the type-1 behavior when the clay mineral content is lower than  $\sim 11.2\%$ . The related reservoirs may apply a fast flowback regime to reduce water lock damage.

If the clay mineral content is neither low nor high, the swelling pressure of clay minerals can exceed tensile strength to induce intergranular microfractures extension (Özkaya 1988, Singh 2016). The intergranular microfractures can develop and connect to one another to form larger cracks visible to the naked eye. The pore structure of rock could change during water imbibition. The T2 spectra that represent pore size tend to increase gradually (figure 12(b)). According to the experimental results of the NTT, LJP and LMX samples, the rocks may have the type-2 behavior when the clay minerals content is about  $20.5\% \sim 30.2\%$ . Overall, the extension of cracks due to water imbibition can enhance reservoir permeability to some extent. Increasing shutting-in periods may contribute to shale gas production after fracturing operations.

If the clay mineral content is very high, the brittle minerals tend to be suspended by soft clay minerals (figure 12(c)). The microfractures cannot develop due to the low brittleness coefficient of the rocks. The high swelling pressure of clay tends to compact and block the matrix pores, inducing water sensitive damage. The T2 spectra that represent pore size tend to decrease gradually. According to the experimental results of the GCG and LYC samples, the rocks may have the type-3 behavior when the clay mineral content is larger than  $\sim 36.8\%$ . Considering strong water sensitive and

lock damage, the fast flowback regime may not significantly improve related reservoir performance. Waterless fracturing may be applied instead of slick water fracturing.

The shift of the T2 peak may result from clay mineral hydration that has significant effects on pore structure, such as the extension of cracks and matrix pore destruction. Therefore, the shift of the T2 peak is accompanied by pore structure changes. The brittle marine shale contributes to the extension of cracks and the plastic continental shale tends to result in pore destruction. The extension of cracks can increase the imbibition rate, while the pore destruction can decrease the imbibition rate. In addition, the changes in pore structures may also change the surface relaxation that affects the shift of the T2 peak. However, few studies have concentrated on the variation of surface relaxation during water imbibition. More experiments should be conducted on surface relaxation to help understand the T2 spectra characteristics in the future.

## 5. Conclusions

A series of NMR experiments were carried out to study the special imbibition characteristics of shale. This work analyzed the potential effects of clay mineral content on gas production. Sandstone, marine, and continental shale were taken into consideration. Our conclusions are as follows:

- (1) For the same type of shale, the water adsorption by clay minerals can act as an additional driving force to enhance the imbibition rate. The more clay mineral there is, the larger the imbibition rate becomes. But continental shale contains more clay minerals and has a larger imbibition rate than marine shale.
- (2) The T2 values of sandstone remain constant and that of shale varies during water imbibition. The T2 values of marine shale increase gradually, indicating the extension of microfractures. The T2 values of continental

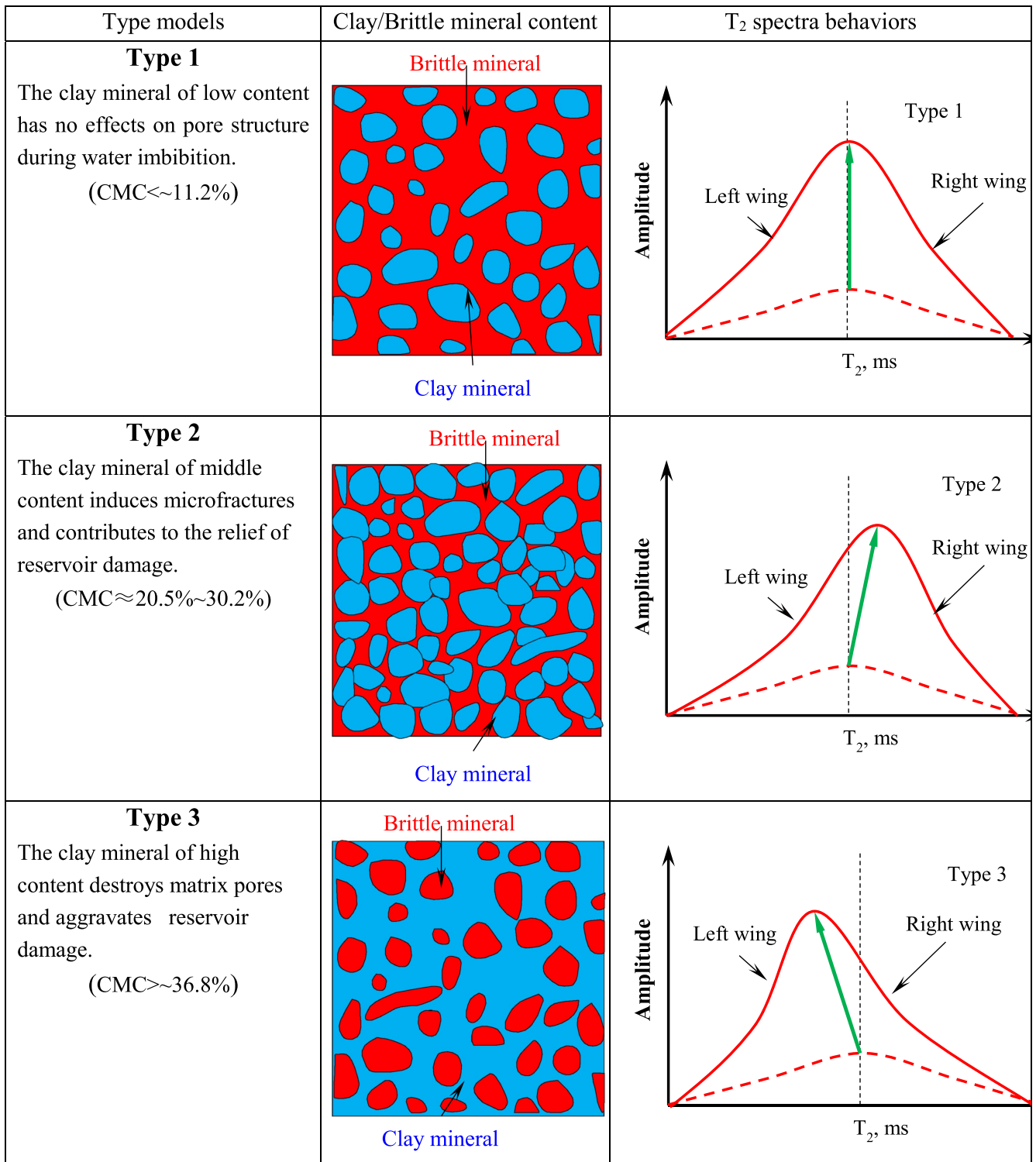


**Figure 12.** Schematic diagram of the type model: (a) low clay content, (b) middle clay content, (c) high clay content. The blue areas represent soft clay minerals, and the red areas represent brittle minerals. CMC indicates clay mineral content.

shale decrease gradually, which suggests that the matrix pores are compacted or destroyed.

- (3) Three models are proposed to analyze the imbibition characteristics for various types of rocks. Compared with continental shale, increasing shutting-in periods is more suitable for marine shale.

## Acknowledgments

The financial support of our shale research program is supported by the National Natural Science Foundation of China under Grant No. 11702296, the National Science and Technology Major Project under Grant No. 2016ZX05046-003,

and the China Postdoctoral Science Foundation under Grant No. 2016M601141.

## ORCID iDs

Liu Yang  <https://orcid.org/0000-0002-4816-5942>

## References

- Cheng C, Perfect E, Donnelly B, Bilheux H Z, Tresmin A S, McKay L D, DiStefano V H, Cai J C and Santodonato L J 2015 Rapid imbibition of water in fractures within unsaturated sedimentary rock *Adv. Water Resour.* **77** 82–9
- Dehghanpour H, Zubair H A, Chhabra A and Ullah A 2012 Liquid intake of organic shales *Energy Fuels* **26** 5750–8
- Dehghanpour H, Lan Q, Saeed Y, Fei H and Qi Z 2013 Spontaneous imbibition of brine and oil in gas shales: effect of water adsorption and resulting micro fractures *Energy Fuels* **27** 3039–49
- Ge H, Yang L, Shen Y, Ren K, Meng F, Ji W and Wu S 2015 Experimental investigation of shale imbibition capacity and the factors influencing loss of hydraulic fracturing fluids *Pet. Sci. Eng.* **12** 636–50
- Gruener S, Hermes H, Schillinger B, Egelhaaf S U and Huber P 2016 Capillary rise dynamics of liquid hydrocarbons in mesoporous silica as explored by gravimetry, optical and neutron imaging: nano-rheology and determination of pore size distributions from the shape of imbibition fronts *Colloids Surf. A* **496** 13–27
- Gomaa A M, Zhang B, Chen J, Qu Q and Nelson S 2014 Innovative use of NMR to study the fracture fluid propagation in shale formation *SPE Hydraulic Fracturing Technology Conf. (The Woodlands, TX, USA, February 4–6)* (Society of Petroleum Engineers) SPE-168619 (<https://doi.org/10.2118/168619-MS>)
- Guo T, Zhang S, Ge H, Wang X, Lei X and Xiao B 2015 A new method for evaluation of fracture network formation capacity of rock *Fuel* **140** 778–87
- Handy L L 1960 Determination of effective capillary pressures for porous media from imbibition data *Pet. Trans. AIME* **219** 75–80
- Hayatdavoudi A, Boamah M A, Tavnaei A, Sawant K G and Boukadi F 2015 Post frac gas production through shale capillary activation *Proc. of the SPE Production and Operations Symp. (Oklahoma City, OK, March 1–5)* (Society of Petroleum Engineers) SPE-173606-MS (<https://doi.org/10.2118/173606-MS>)
- Hu Q H, Ewing P R and Dultz S 2012 Low pore connectivity in natural rock *J. Contam. Hydrol.* **133** 76–83
- Lam C H and Horváth V K 2000 Pipe network model for scaling of dynamic interfaces in porous media *Phys. Rev. Lett.* **85** 1238–41
- Lucas R 1918 Rate of capillary ascension of liquids *Kolloid Z.* **23** 15–22
- Makhanov K, Dehghanpour H and Kuru E 2012 An experimental study of spontaneous imbibition in Horn River shales *SPE Canadian Unconventional Resources Conf. (Calgary, Alberta, Canada)* (Society of Petroleum Engineers) SPE-162650 (<https://doi.org/10.2118/162650-MS>)
- Meng M, Ge H, Ji W and Wang x 2016 Research on the auto-removal mechanism of shale aqueous phase trapping using low field nuclear magnetic resonance technique *J. Pet. Sci. Eng.* **137** 63–73
- Özkaya L 1988 A simple analysis of oil-induced fracturing in sedimentary rocks *Mar. Pet. Geol.* **5** 293–7
- Odumabio S M and Karpyn Z T 2014 Investigation of gas flow hindrance due to fracturing fluid leakoff in low permeability sandstones *J. Nat. Gas Sci. Eng.* **17** 1–12
- Singh H 2016 A critical review of water uptake by shales *J. Nat. Gas Sci. Eng.* **34** 751–66
- Wang J and Raman S S 2015 An investigation of fluid leak-off due to osmotic and capillary effects and its impact on micro-fracture generation during hydraulic fracturing stimulation of gas shale *EUROPEC 2015 (Madrid, Spain, 1–4 June)* (Society of Petroleum Engineers) SPE-174392-MS (<https://doi.org/10.2118/174392-MS>)
- Washburn E W 1921 Dynamics of capillary flow *Phys. Rev.* **17** 273–83
- Xu H, Tang D, Zhao J and Li S 2015 A precise measurement method for shale porosity with low-field nuclear magnetic resonance: a case study of the carboniferous-Permian strata in the Linxing area, eastern Ordos Basin, China *Fuel* **143** 47–54
- Yang L, Ge H, Shen Y, Zhang J, Yan W, Wu S and Tang X 2015 Imbibition inducing tensile fractures and its influence on *in situ* stress analyses: a case study of shale gas drilling *J. Nat. Gas Sci. Eng.* **26** 927–39
- Yang L, Ge H, Shi X, Cheng Y, Zhang K, Chen H, Shen Y, Zhang J and Qu X 2016 The effect of microstructure and rock mineralogy on water imbibition characteristics in tight reservoirs *J. Nat. Gas Sci. Eng.* **22** 1–11